Reprinted from:

White, R. S., Spitzer, R., Christie, P. A. F., Roberts, A., Lunnon, Z., Maresh, J. & iSIMM Working Group (2005). Seismic imaging through basalt flows on the Faroes Shelf, in Ziska, H., Varming, T. & Blotch, D. (eds.), *Faroe Islands Exploration Conference: Proceedings of the 1st Conference, Annales Societatis Scientiarum Færoensis (Faroese Society of Sciences and Humanities),* Supplementum **43**, Tórshavn, pp. 11−31.

Seismic Imaging through Basalt Flows on the Faroes Shelf

ROBERT S. WHITE[1*], ROMAN SPITZER[1], PHILIP A.F. CHRISTIE[2], ALAN ROBERTS[1], ZOË LUNNON[1], JENNIFER MARESH[1] AND ISIMM WORKING GROUP[3]

1: Bullard Laboratories, Madingley Rd., Cambridge CB3 0EZ, UK.
*Email: rwhite@esc.cam.ac.uk; Tel: +44 1223 337187; Fax: +44 1223 360779
2: Schlumberger Cambridge Research Ltd., High Cross, Madingley Road, Cambridge CB3 0EL, UK.
3: iSIMM Working Group comprises N.J. Kusznir, R.S. White, A.M. Roberts, P.A.F. Christie, R. Spitzer, N. Hurst, Z.C. Lunnon, C.J. Parkin, A.W. Roberts, V. Tymms and D. Healy.

Abstract

Massive magmatism occurred on the North Atlantic margins when the continents broke apart in the presence of the Iceland mantle plume. The extrusive basalts on the Faroes Shelf create a considerable problem for seismic imaging by causing extensive scattering from the multiple lava flows and by attenuating the higher frequencies in the seismic signal. We have made considerable advances in imaging through the basalts and into the underlying sediments and basement by focussing on the generation and recording of low-frequency energy centred on ~10 Hz and by making use of the additional information available from long-offset data. We show how such low frequency seismic signals can be generated and recorded, and how long-offset data can be acquired using currently available technology. We outline the processing and imaging strategies we have developed and show results that illustrate these techniques from two recent seismic experiments (FLARE and iSIMM), shot across the Faroes Shelf and adjacent continental margin. Combination of normal incidence and wide-angle seismic data, together with the use of sources and receivers tuned to the low frequencies required for intra- and sub-basalt penetration enable us to see structure both within and below the basalts.

Introduction

Extrusive igneous rocks dominate the northwestern flank of the Faroes-Shetland Basin and the Faroes Shelf. Flood basalts created at the time of breakup between the Faroe Islands and east Greenland extend over 250,000 km^2, at least 40,000 km^2 of which lie in the Faroe-Shetland Basin (Naylor *et al.*, 1999). They attain a thickness of more than 7 km on the Faroe Islands themselves, and extend some 150 km eastwards from the islands to feather out in the Faroe-Shetland Trough (Figure 1). Their thickness and distribution in the Faroes area has been reported by White *et al.* (2003) and Sørensen (2003). The volcanic rocks in the Faroes region are part of a much larger igneous province with up to 10 million km^3 of rock generated when the North Atlantic Ocean opened above a thermal anomaly in the mantle caused by a mantle plume which currently lies beneath Iceland (White and McKenzie, 1989; Eldholm and Grue, 1994). This larger igneous province extends from the northern tip of Norway to the southern part of Rockall Plateau on the eastern side of the North Atlantic, and down the east coast of Greenland on the conjugate margin.

Regionally, both the sediment supply and the availability of accommodation space within the Faroes-Shetland Basin through the Paleocene and Eocene were controlled primarily by the uplift caused by the Iceland mantle plume beneath the

Faroe Islands Exploration Conference: Proceedings of the 1st Conference.
Annales Societatis Scientiarum Færoensis, Supplementum 43, Tórshavn, 2005: 1-7

lithosphere and by the volcanism in the Paleocene. So there is a complex and intimate link between the rifting, subsidence, sedimentation and igneous histories of the Faroes region (Doré *et al.*, 2002).

Early Palaeocene sedimentation in the basin was controlled initially by the underlying end-Cretaceous fault-induced topography (Ebdon *et al.*, 1995), until these fault basins were infilled. Subsequently a period of deep-water fan sand progradation across the basin developed, attributed by White and Lovell (1997) to enhanced erosion and base level changes caused by uplift of the shelf and hinterland by the proto-Icelandic mantle plume. Following the end of the Paleocene rifting, an abundant supply of clastic material, derived from the uplifted Scottish Highlands, built two major progradational packages out across the basin, the Lamba and Flett Formations. Clinoforms 500 m high in the Lamba, and at least 300 m high in the Flett Formation indicate the paleo-water depth and show the scale of the depositional systems. The major extrusive igneous activity which generated the first basalts on the Faroes commenced during deposition of the Flett Formation (White *et al.*, 2003).

The end of the basalt extrusion is marked by the culmination of a major uplift event and development of a regional unconformity, which forms the base to the overlying Balder Formation. The Balder Formation itself progressively onlaps the top basalt surface to the northwest as marine transgression proceeded and deep marine conditions were re-established across the basin in the Lower Eocene. A suite of sills in the centre of the Faroe-Shetland basin is thought to have been intruded mainly around the time of the Balder Formation (Smallwood and Maresh, 2002).

Overall, the Eocene and following periods were dominated by post-rift thermal subsidence. This general subsidence during the Cenozoic was punctuated by several periods of both local and regional uplift (Nadin *et al.*, 1997). A number of compressional events formed inversion structures in the Faroe-Shetland Basin between the late Paleocene and the Miocene, events which are now reflected in the shape of the top basalt surface (Boldreel and Andersen, 1993).

The extrusive lavas pose a particular problem for seismic imaging through to the underlying, possibly prospective, sediments and basement structure. In this paper we discuss the main causes of these problems. We show that by focussing on the production and recording of low-frequency seismic energy, improved sub-basalt images can be obtained. We then discuss practical ways of increasing the low-frequency response of seismic profiling systems. Another helpful approach for sub-basalt imaging is to record seismic data to very long offsets, which provide additional refractions and wide-angle reflections at angles approaching the critical angles. By using new processing techniques, these wide-angle arrivals can be used to help identify deep reflections from the base of thick basalt sequences and the underlying structure.

We illustrate these techniques using data from two novel surveys on the Faroes Shelf. The first

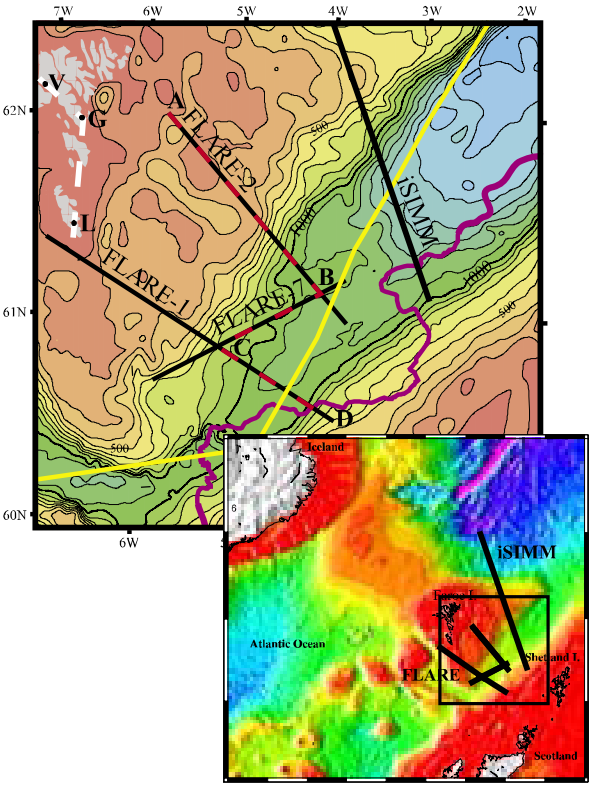

Figure 1. Map showing location of long-offset two-ship FLARE and single-ship, 12 km iSIMM profiles used in this paper. Main map covers the same area as basalt thickness map in Figure 9. Purple line marks southeastern limit of Tertiary basalt flows. Yellow line marks boundary between UK and Faroes waters. Bathymetric contours every 100 m. Red dashes mark the location of the composite seismic profile illustrated in Figure 8. Borehole locations marked by G - Glyvursnes; L - Lopra 1/1A; V – Vestmanna with white dotted line joining them showing line of cross-section in Fig. 2. Inset shows regional setting, area of main map and complete length of iSIMM profile.

is the Faroes Large Aperture Research Experiment (FLARE), which was acquired by the Amerada Hess Limited Partner Group. By using flip-flop firing from two seismic vessels, each towing streamers, profiles with offsets of up to 38,000 m were acquired. The second is the iSIMM (integrated Seismic Imaging and Modelling of Margins) profile, which extends 400 km across the northern Faroes Shelf and continent-ocean boundary (Figure 1).

The Requirement for Low Frequencies to Penetrate Basalts

Layered sequences of lava flows act as effective high-cut filters to seismic energy transmitted through them. This means that the higher frequency energy is attenuated rapidly, so most reflections from sub-basalt horizons are therefore rich only in the lower frequency energy.

There are now several good determinations of the effective seismic quality factor, Q, from basalt sequences on the Faroe Islands themselves, and from elsewhere in the North Atlantic, including the northern Rockall Trough (Maresh *et al.*, 2003). In addition, there are some measurements from both sub-aerial (Columbia River basalts) and submarine (Juan de Fuca Ridge) extrusive lavas elsewhere (Table 1). Most of the measurements of Q have been made by spectral analyses of seismic energy recorded from vertical seismic profiles (VSPs) in boreholes. The spectral ratio method (Toksöz *et al.*, 1979), for estimation of Q works by comparing the spectrum of the waveform incident on the basalt layer with the spectrum after transmission through the basalt, so it is dependent on the incident waveform having a broad spectrum to start with.

Strictly speaking, the processes causing loss of the higher frequency energy are not primarily absorption, because massive basalt is not strongly absorptive. For massive basalts, the intrinsic Q is typically within the range 100–400. However, the effective Q values derived by spectral analysis provide a convenient measure of the effect of the basalt layers on the transmitted energy. The effective Q probably comprises a small component of intrinsic absorption, and a larger effect from scattering. The scattering disperses the energy, and preferentially scatters the higher frequency components for the velocity structure of typical lava flow sequences, and so removes it from the coherent first arriving reflections.

Part of the scattering is caused by the strongly layered nature of the basalt flows. Typically an individual lava flow has a massive interior, with vesiculated, weathered or even rubbly tops that exhibit lower seismic velocities (Planke, 1994). There may also be soil or sediment horizons between the flows which often have even lower seismic velocities. Since the individual flows are usually relatively thin (a few metres to a few tens

Location	Q	Reference
Columbia Plateau Basalts	48	Pujol and Smithson, 1991
Upper Basalt Series, Vøring Plateau, Norwegian Sea	~40	Rutledge and Winkler, 1987
Juan de Fuca Ridge, Pacific Ocean	20–50	Jacobsen and Lewis, 1990
Tertiary basalts, Northern Rockall Trough, North Atlantic	15–35	Maresh *et al.*, 2003
Lower Basalt Series, Lopra Borehole, Suðuroy, Faroe Is.	35	Christie *et al.*, in press
Upper and Middle Basalt Series, Glyvursnes borehole, Streymoy, Faroe Is.	~10–45	Shaw *et al.*, 2004

Table 1. Summary of Effective Seismic Quality Factor, Q, from Basaltic Flow Sequences

of metres thick), a typical stack of lava flows may contain hundreds of sub-horizontal interfaces with large impedance contrasts. These readily cause numerous intra-basalt multiples, which scatter the energy (Christie *et al.*, in press).

Within the Faroe Islands themselves, three scientific boreholes penetrate portions of the Lower, Middle and Upper Basalt formations. These are the Lopra, Vestmanna and Glyvursnes boreholes (Figure 2), and all three have been extensively cored, logged and studied by VSPs and wide-angle seismic experiments (Japsen *et al.*, 2005). Quality factors of ~10–45 have been reported (Christie *et al.*, 2002, and in press; Shaw *et al.*, 2004), with typical values being 35–40. There is some indication in the Glyvursnes borehole that Q increases with depth, which may partly be caused by the difference between the Upper and the Middle Basalt formations (Figure 2), and partly due to increasing depth beneath the surface correlating with a smaller percentage of open pore space and fractures. In offshore basalt sequences on the Faroes Shelf, velocity gradients ranging from 0.1 to 0.7 km/s per km are found (Fliedner and White, 2001a; Spitzer *et al.*, 2004). Such velocity gradients are also indicative of a decrease in the amount of cracking and pore space with depth which would tend to correlate with an increase of Q with depth.

In Figure 3a we show theoretical calculations of the effect on the frequency content of waveforms that have undergone two-way transmission at normal incidence through a 1-km-thick basalt sequence with an average seismic velocity of 4 km/s for a range of different realistic values of Q. The incident wave has an amplitude of unity at all frequencies and this diagram shows the effect of attenuation without including any other factors that might affect the amplitude, such as geometric spreading or interference between reflections off different interfaces. The high frequencies are extremely rapidly attenuated. For example, if Q is 25, then a 10 Hz signal will lose slightly less than half of its amplitude in two-way transmission through a 1-km-thick basalt layer, while a 50 Hz signal will lose 96% of its amplitude. Or, in other words, a perfect reflection from the base of the basalts will retain 53% of the incident amplitude for a 10 Hz signal, but only 4% of the incident amplitude for a 50 Hz signal.

So if we wish to see seismic reflections from beneath thick basalts, there is little alternative than to use low frequencies. The unfortunate corollary is that the low frequencies limit the resolution, but it is better to lose some resolution and to obtain interpretable sub-basalt reflections than to use higher frequencies and as a result to record no reflected sub-basalt energy above the noise levels.

Generation and Recording of Low-Frequency Seismic Energy

In the context of imaging sub-basalt structure, seismic sources rich in energy at about 10 Hz are required, although it is also important to retain as great a bandwidth as possible to ensure maximum resolution until the signal becomes swamped by noise. Conventional airgun sources, typically peak-tuned, towed at 5–8 m depth, with volumes of ~70 litres (c. 4,000 cu. in.), and centre frequencies of ~50 Hz still produce some energy at low frequencies, and have proven to be capable of penetrating at least thin sections of basalts. The FLARE profiles provide an example of this (White *et al.*,

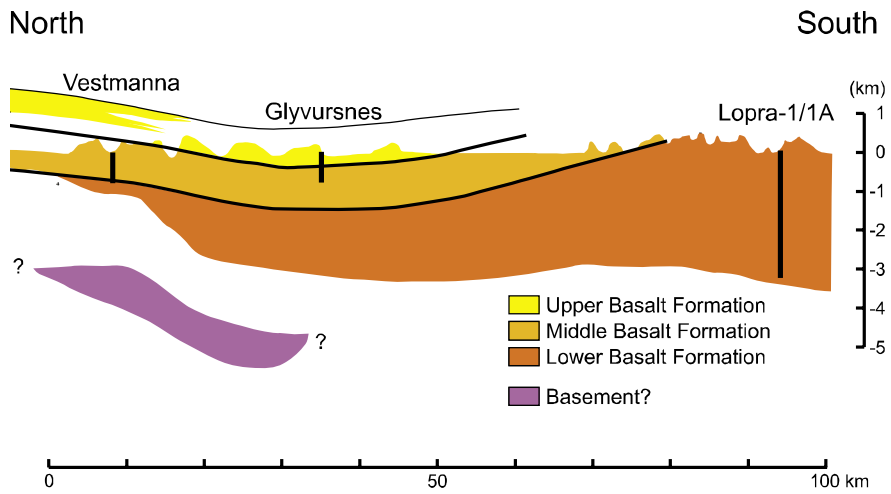

Figure 2. Stratigraphic position of boreholes through basalt on the Faroe Islands, superimposed on cross-section passing through the boreholes (modified from Waagstein, 1988). For location of cross-section and boreholes, see Figure 1.

2003), although the signal-to-noise ratio and hence the confidence of interpretations of weak sub-basalt reflectors are much poorer than with sources designed to be rich in low frequencies (Lunnon *et al.*, 2003; Spitzer *et al.*, 2004).

Using conventional airgun technology there are three main ways of producing low frequencies with significant energy at ~10 Hz using marine sources.

Use Big Airguns

At a given depth and air pressure, the larger the airgun volume, the lower the frequency of the bubble pulse. So the simplest way to produce lower frequencies is to increase the chamber volume. This is not completely trivial, because the larger the chamber, the more difficult it is to evacuate the air quickly through the vents once the gun is triggered. But this concept has been used by Ziolkowski *et al.* (2003), to produce low-frequency energy centred at 20 Hz by using 'large' chambers (the chamber size is not specified in their paper). The disadvantage of using a limited number of very large guns is that the source may become rather monochromatic, which can be deleterious to resolution. But it is arguable that the low-pass filtering effect of thick basalt flows only allows a limited range of frequencies to penetrate the basalt in any case, so this may be less of a drawback than it at first appears.

A more conventional way to increase the overall airgun volume is to use standard arrays of airguns, but with more guns, perhaps biased toward the larger conventional chamber sizes. Using this approach, the FIRE (Faroes-Iceland Ridge Experiment) profiles shot in 1994 across the continental margin northwest of the Faroe Islands achieved a total volume of 153 litres (9,324 cu. in.), with 48 guns, the largest of which was 8.2 litre (500 cu. in.). The source was towed at a depth of 10 m. Good arrivals were recorded at ranges up to 160 km after propagation through the basaltic crust and upper mantle beneath the 35-km thick Faroe-Iceland Ridge (White *et al.*, 1996; Smallwood *et al.*, 1999; Staples *et al.*, 1999). One of the disadvantages of simply increasing the power of the source array, however, is that the source-generated 'noise' due to multiples and water-wave 'wrap-round' (McBride *et al.*, 1994) is also increased. It may then become necessary to increase the interval between shots to allow the source-generated noise to decay, and this of course has the deleterious effect of reducing the fold of cover.

Tow Airguns Deep

The sea-surface acts as an almost perfect reflector, because there is such a large impedance contrast between water and air. It also causes a phase reversal in the downward reflected wave. Since airgun arrays radiate energy in all directions, the downward-travelling wave which is used for seismic imaging is supplemented by the surface reflected wave, which is phase-inverted and delayed in time by an amount dependent on the depth of the source beneath the surface. Constructive interference occurs if the source is towed at a depth of one quarter of a wavelength. So, for example, since the speed of sound in water is close to 1500 m/s, the optimum depth for constructive interference is 19 m at 20 Hz, or 38 m at 10 Hz.

However, there is a counter-effect of increasing the tow depth of airguns. Because the ambient pressure is higher at greater depth, the frequency of oscillation of the bubble pulse increases as a gun of any given volume is towed deeper. So there is a trade-off in increasing the tow depth of airguns between enhancing the constructive interference from the sea-surface reflection by going deeper, while preventing the primary bubble frequency increasing too much by not going too deep.

In practice, this trade-off is optimized at an airgun tow-depth of 15–20 m, and several surveys designed for low frequencies have used arrays at such depths. They include the survey reported by Ziolkowski *et al.* (2003), mentioned above and the FLARE survey, from which we show extracts later in this paper, which both used airgun depths of 15 m. The iSIMM profiles, which are also discussed later used 18–20 m airgun depths (Lunnon *et al.*, 2003). An airgun array depth of up to 20 m is operationally attractive because it can usually be accommodated within the normal towing arrangements of the airgun array on a seismic acquisition vessel. It is also worth noting that although the peak enhancement at 19 m depth occurs at a frequency of 20 Hz, which is somewhat higher than our optimum of 10 Hz, as Figure 3b shows, the sea surface reflection enhances the source signal over a bandwidth of 2.32 octaves up to the first notch at which destructive interference reduces the signal

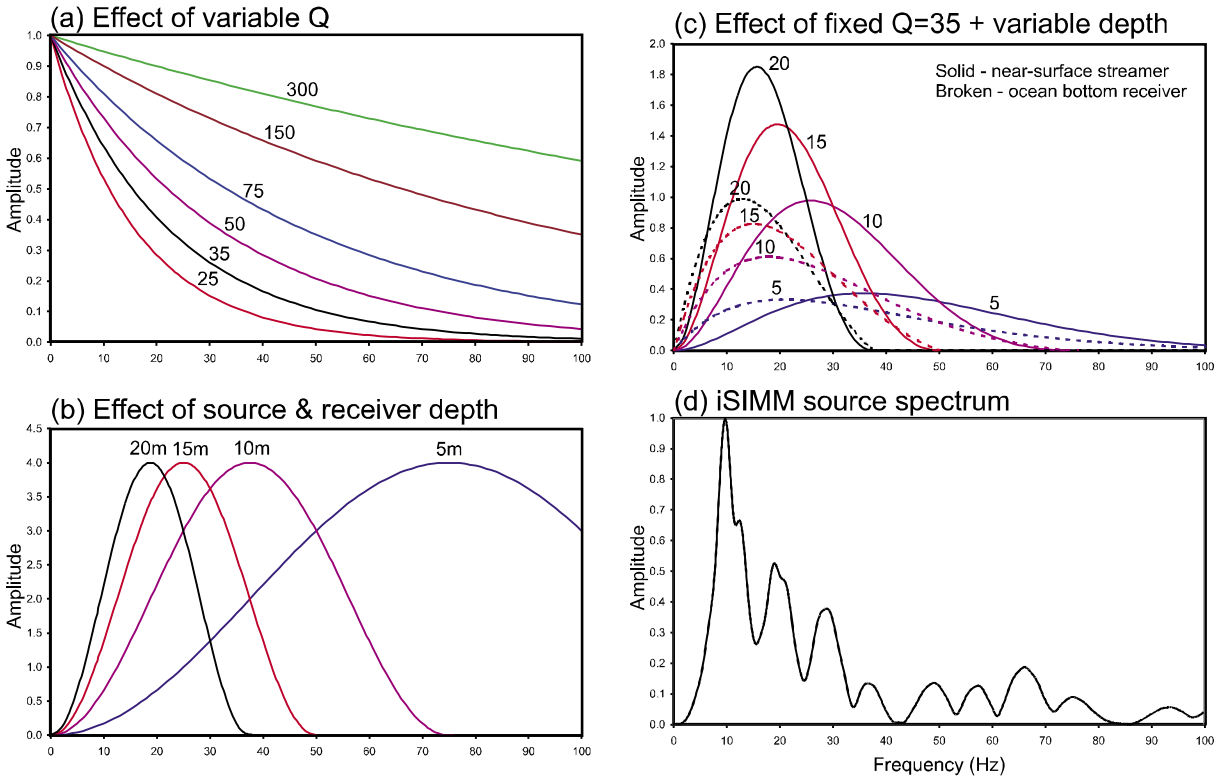

Figure 3. Theoretical calculation of effect of quality factor Q, and depth of source and receiver on frequency-dependent amplitudes of seismic waves passing through basalt. All calculations are for two-way transmission at normal incidence through a 1 km thick basalt layer with an average seismic velocity of 4 km/s and do not include any other sources of amplitude variation, such as geometric spreading or interference between multiple reflectors. Incident wave has an amplitude of 1.0 across all frequencies from 0–100 Hz. Panels (**b**) and (**c**) only show the response up to the first notch where destructive interference occurs. (**a**) effect of varying Q; (**b**) effect of varying the source and receiver depth (both kept identical); (**c**) effect of holding Q fixed at the geologically typical value of 35 (black line in Fig. 3(**a**)), solid lines show effect of different source and receiver depths (both identical), broken lines show effect of different source depths with a deep water ocean bottom receiver; (**d**) far-field source spectrum including the source ghost used for iSIMM seismic reflection profiles, with bubble-tuning and source at 18 m depth.

to its minimum, at whatever depth the source is towed (Lunnon *et al.*, 2003). So towing the source deeper than the conventional depth of 5–8 m always enhances the low-frequency response. At 19 m depth there is a significant enhancement at 10 Hz in addition to the maximum enhancement at 20 Hz.

There is a marked effect of combining the low-frequency filtering effect of the basalts with the tow depth of the source and receivers. This is shown in Figure 3c, where we assume a typical value of 35 for the quality factor, Q based on observational results from basalts in the Rockall and the Faroes regions (Table 1), and demonstrate the interaction of this with the low-frequency enhancement of towing deep. The overall result is that the window for energy to propagate through the basalts is centred on the low-frequency part of the spectrum, so to make full use of this it is important to tune the source to match as far as possible the frequency pass band of the basalts, while maintaining as large a bandwidth as possible for the source to optimise the achievable resolution.

Use Bubble Tuning rather than Peak Tuning

A novel way to enhance the low frequency energy in an airgun source is to set the individual firing delays on the airguns such that the first bubble pulse of the different airguns is enhanced rather than to use the conventional firing method which enhances the first peak. This was first suggested by Avedik *et al.* (1993), based on earlier work by Safar (1980), together with a refinement that different sized airguns might be towed at different depths so as to individually optimize the enhancement of their bubble frequencies by towing close to their individual optimum depths for reinforcement by the sea-surface reflection. In designing

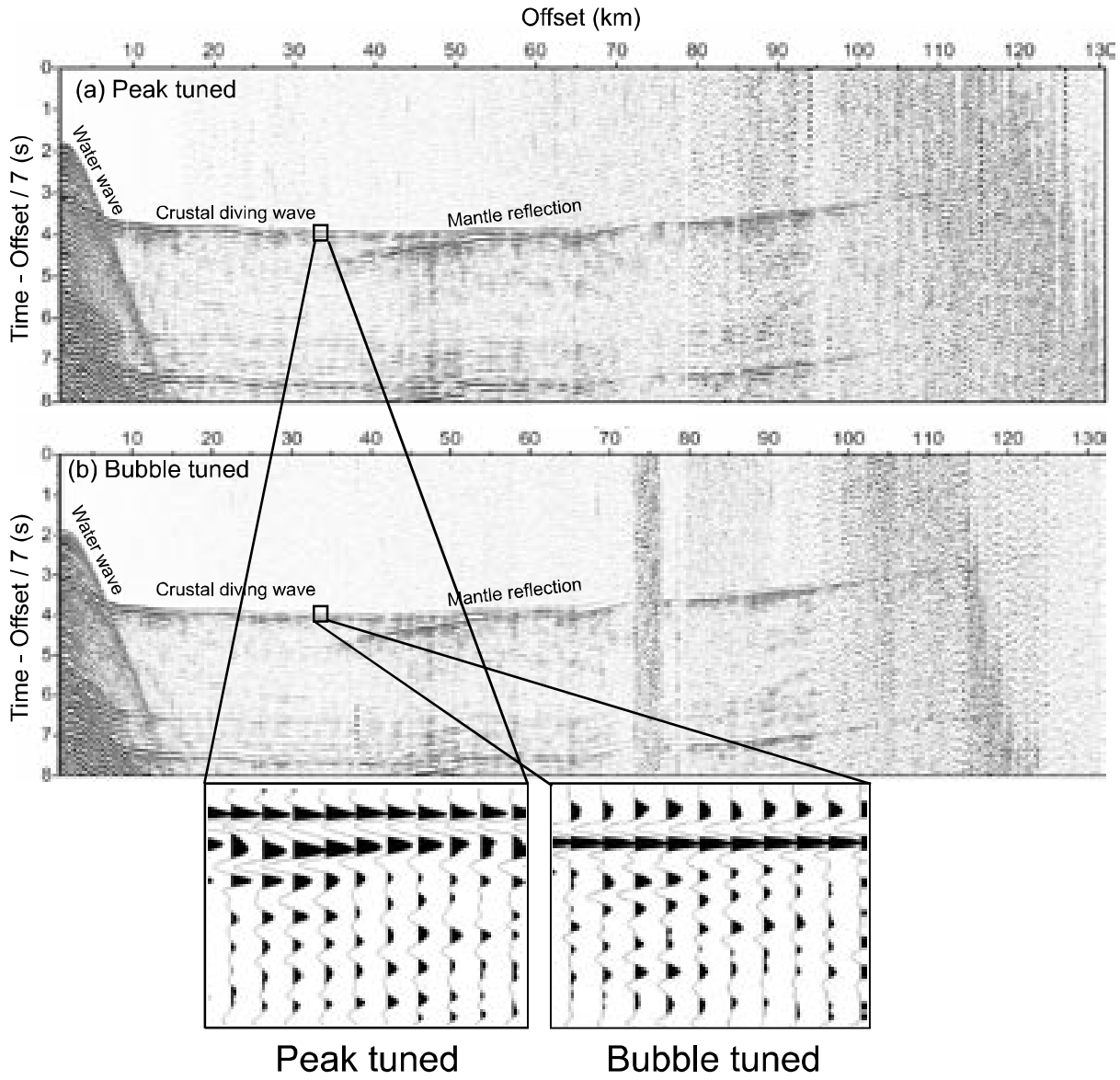

Figure 4. Receiver gathers from an OBS on the iSIMM profile to show the difference between (**a**) peak tuning, and (**b**) bubble tuning. Location of OBS is shown on Figure 10, with shots fired toward the southeast. Both profiles use the same airgun configuration of a 104 litre, (6,360 cu in.) array of 14 guns towed at 20 m depth, with the only difference being the tuning method. Note the sharp wide-angle Moho reflection, which attains high amplitude beyond 35 km offset as the critical distance is approached. Data are band-pass filtered 3–18 Hz, and only every second trace is displayed after a running trace mix. Reduction velocity (equivalent to linear moveout) of 7 km/s means that arrivals with a phase velocity of 7 km/s are horizontal in this display. Enlargements show the more compact nature of the bubble-tuned source. Figure after Roberts *et al.* (in press).

the source for the iSIMM profiles we took a similar approach of tuning on the first bubble pulse. From far-field monitoring of the wavefield using vertical arrays we have shown that the iSIMM bubble-tuned source contains significantly more low-frequency energy than an identical source fired with conventional peak-pulse tuning (Lunnon *et al.*, 2003). From repeat firing into fixed ocean bottom seismometers deployed along the iSIMM profile using first peak tuning and then bubble tuning, we have also found that the long-range propagation of low-frequency seismic energy is markedly better for the bubble-tuned sources (White *et al.*, 2002; Roberts *et al.*, in press). Another advantage of the bubble-tuned source, reported by Lunnon *et al.* (2003), is that after it has propagated through the earth filter produced by the subsurface, the bubble-tuned waveform is more compact than the peak-tuned waveform, so is capable of producing better resolution of deep structure, a characteristic which is of particular importance with wide-angle ocean bottom seismometer data (Figure 4).

The iSIMM source for the Q-streamer profile data, from which we show extracts later, used a 48-gun, 167 litre (10,170 cu in.) array towed at 18 m depth with bubble-tuning (White *et al.*, 2002; Hoare *et al.*, this volume). Individual airgun chamber sizes ranged from 1.7 to 4.8 litres (105 to 290 cu in.), with some of the guns clustered to produce an effective volume of 9.6 litres (580 cu in) from the clusters. The resultant waveform is rich in low frequencies (Figure 3d), producing considerable energy in the window which allows propagation through the basalts and making it well matched to the geological requirements. Operationally, an advantage of bubble-tuning is that it can use conventional airgun arrays with just a minor change to the firing control parameters.

Source Designature

Whatever source is used, the Common Mid-Point stack is improved if shot-by-shot designature is applied before stacking. This is better than a purely statistical approach to source deconvolution which optimizes some chosen statistical measure, and is also better than the normal assumption that the source signature is invariant along the profile. However, there is a practical problem in recording the far-field signature of every shot. One approach is to tow a hydrophone at depth to record the outgoing waveform from each shot. This is difficult to do because at a normal acquisition ship speed of about 5 knots, it is not easy to hold a hydrophone both at sufficient depth, and sufficiently close to the ship to record the downgoing far-field waveform. There is, in addition, often a practical problem in that the water depth may be insufficient to allow recording of the far-field waveform in the water column. Another experimental approach for assessing the far-field waveform for each shot, reported by Hobbs and Jakubowicz (2000), is to fire a small reference source immediately prior to the main airgun array, and from that to calibrate the main source using the seabed reflection as a signal common to both.

An alternative approach to shot designature is to record the waveforms at individual pressure sensors or accelerometers close to each airgun, and then to reconstruct the far field source signature from these individual near-field measurements (Ziolkowski *et al.*, 1982). This approach was used for the iSIMM towed streamer profiles shown here, using calibrated sensors near to each gun. An advantage of shot-by-shot designature is that small changes in the airgun source can be accounted for on every shot. In the case of the bubble-tuned, deep-towed source, we had no prior calibrated library signature and so the use of shot-by-shot signature monitoring was a key enabler in deconvolving the complex source signature into a standard, simple wavelet for further processing.

Receiver Optimisation

The major control which can be applied to the normal streamer configuration so as to enhance the low-frequency response is to tow it deeper, as the sea surface ghost enhances the low-frequency response. In the iSIMM profiles displayed in this paper, the source and streamer were both towed at 18 m below the sea surface, because this doubles the effect of constructive interference. At the frequency corresponding to the optimum depth the amplitude is increased by a factor of four (Figure 3b). An additional benefit of towing the streamer deep is that it is less susceptible to wave noise from rough seas. Since the wave noise is generally at the low-frequency end of the spectrum, this proves to be an important benefit because it gives a much lower noise level in precisely that part of the spectrum that we have to use for detecting sub-basalt returns.

If bottom receivers are available, either as ocean bottom seismometers or as a bottom cable, the bandwidth available is further enhanced, because the signal at the receiver detectors (at least in deep water), do not suffer the notches created by the sea-surface interference. This is demonstrated in Figure 3c: the solid lines show the effect of towing both the source and the receiver at a range of (identical) depths, while the broken lines show the response of a seabed receiver, with only the source at varying depths. Although the amplifying effect of the sea-surface reflection due to constructive interference is greater when the receiver is near the surface (solid lines), the bandwidth is considerably greater when the receiver is on the sea bottom (broken lines). Since the limiting noise level is often signal-generated (multiples and scattering), rather than the ambient background level, the absolute signal level is probably of less importance than the ability to record low frequencies, so the greater bandwidth available from a bottom cable is likely

to have a highly beneficial effect on sub-basalt imaging.

Long-Offset Acquisition

Acquisition of wide-angle data, which requires long offsets, provides considerable additional information that is useful for sub-basalt imaging. In this section we first examine the theoretical basis for this assertion and the types of additional or supplementary information that can in principle be derived from wide-angle data, then we discuss practical ways of acquiring long-offset data, and finally show examples of its use in practice in the Faroes region.

In almost all conventional processing of multichannel seismic reflection profiles, one of the first steps is to mute all the energy outside the water-wave cone. This is partly because a large part of this energy at larger offsets comes from diving waves (sometimes called refractions), with close to linear moveout. If they were to be included in the normal hyperbolic moveout correction that is used in stacking the data, they would not stack properly (because they have linear rather than hyperbolic moveout), and so would generate coherent noise on the stacked section. A further problem is that at large offsets the wide-angle reflections from closely-spaced layers, such as those in sediments, converge with increasing offset. When these arrivals are brought back to normal incidence along a hyperbolic moveout curve, they are stretched. If the stretch becomes unacceptably large this degrades the image, so for this reason, too, a mute is often applied to the longer offset data. However, there is considerable information, particularly on the velocity field, in these wide-angle arrivals, so if they are used in conjunction with the better imaging characteristics of the conventional near-offset field, the combined result is both improved imaging and a better understanding of the sub-surface geology.

Theoretical Considerations

The resolution of the stacking velocity in deeper parts of conventional seismic profiles decreases with increasing depth, simply because the moveout of the hyperbolic reflections decreases. At wide angles the velocity resolution improves markedly, partly because diving waves are travelling sub-horizontally and so have much greater moveout with offset than do the near offset reflected waves, and partly because the increased spatial recording aperture of long-offset data provides a larger distance over which to record moveout. There is, however, another significant effect which is of particular importance in sub-basalt imaging, especially when basalt layers overlie sediments with lower seismic velocities. This is that the low-velocity sediments beneath basalts produce a distinctive and easily recognised step-back in the travel times of diving waves as they pass through the low-velocity layer. This is demonstrated in Figure 5, which is a full-waveform synthetic seismogram from a simple 1-D velocity model with a 1.5 km thick basalt layer. A step-back of about 1 sec in the first arriving energy occurs at about 20 km offset. The ray-diagram in the lower panel of Figure 5 shows the reason for this. As the rays (shown in green on Figure 5) pass through the base of the basalts they are refracted away from the normal by the lower underlying velocities, and are only refracted back toward the surface when they enter the higher velocity material of the basement.

The size of the travel-time step-back is determined by the product of the thickness of the low-velocity zone and its velocity, and the two cannot be calculated independently just from the magnitude of the step-back. However, on long-offset data the moveout of the top-basement reflection (solid green line on Figure 5) may be used to determine the sub-basalt sediment velocity and hence its thickness.

The synthetic seismogram in Figure 5 also illustrates another common problem with sub-basalt imaging, which is that there is a great deal of multiple and mode-converted energy present. This is a very simple 1-D model, yet contains many non-primary arrivals: in the real world with laterally varying structure, the complexity of such arrivals only increases. But this example also illustrates another important feature of long-offset arrivals: the first arriving energy is always a primary p-wave, and not a multiple. This means that we can have confidence in using these arrivals to identify primary features of the profile. As discussed later, our approach is to migrate these wide-angle arrivals back to normal incidence, and to use them to 'tag' reflectors that we can then image with better

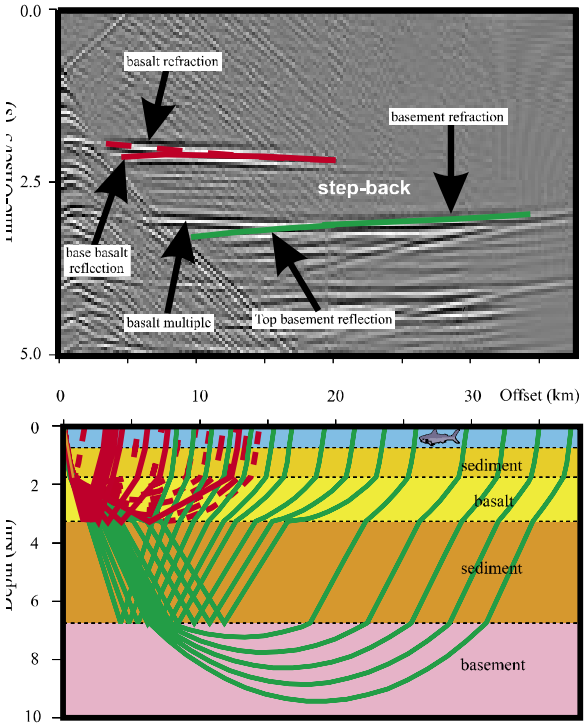

Figure 5. Synthetic seismogram calculated using the full waveform reflectivity response (Fuchs and Müller, 1971), showing the main arrivals and corresponding raypaths that constrain the thickness and velocity of the basalt and of the sub-basalt sediment, modified from White *et al.* (2003). Broken red rays are diving waves through the basalts and solid red rays are reflections off the base of the basalts. Green rays are diving waves through the basement and reflections off the top of the basement. Note the step-back of about 1 s in first arrivals visible at an offset of about 20 km, caused by the low-velocity sediments lying beneath the high-velocity basalt flows. Travel times are reduced with a linear moveout of 5 km/s.

resolution from the near-offset data, having confidence that they are not multiples.

Travel Time Tomography

From the travel times alone, the gross structure can be derived by ray-tracing through a model of the velocity field and iterating the model until there is a satisfactory fit between the calculated and observed travel times. There are several forward modelling and inverse ray-tracing programs that can be used for this, some of which use only first arrivals and others of which also accommodate second arrivals and reflections. This is generally a labour-intensive technique, because it depends on identifying and picking arrivals from coherent phases. There is always the possibility of a trade-off between vertical and lateral variations in velocity structure. Therefore the velocity model is constrained best where there are multiple crossing ray-paths. An example of this is shown in Figure 6, from the FLARE-1 profile (location shown in Figure 1). These data were from multi-pass, two-ship profiles, with maximum offsets of 38 km (White *et al.*, 1999), and provide a first look at the structure beneath the basalts that flowed east from the rift zone near the present location of the Faroe Islands toward the Faroe-Shetland Trough. The crossing ray-paths constrain the structure down to the top of the acoustic basement rocks (probably here of Cretaceous age by analogy with rocks drilled on the eastern flank of the Faroe-Shetland Trough) beneath the basalts. This does not provide detailed structural information on the sub-basalt sediments, but it is sufficient to demonstrate their presence and approximate thickness. It also provides velocity information that can be used for pre-stack depth migration of seismic profile data along the same line.

Another aspect of long-offset data is that the depth of good resolution is limited by the maximum offsets to which data are recorded, as illustrated in Figure 6a. In the particular profile shown in Figure 6, we also deployed 3-component land stations on the Faroese island of Suðuroy, straddling the Lopra borehole and crossing the island (Richardson *et al.*, 1999). The longer-offset arrivals recorded by these fixed stations detected Moho reflections at large range, which allow the depth of the Moho to be constrained, at least at the reflection points.

Integration of Seismic and Other Data

Although seismic surveying remains the technique of choice for imaging the sub-surface, regional extrapolation is possible using other potential field measurements such as gravity, magnetic field and electromagnetic sounding. For example, the Moho has been extrapolated along the profile in Figure 6 using gravity data and the local constraint from the land recording of a wide-angle Moho reflection over a short length of the profile. Magnetic anomaly measurements are also useful for mapping the basaltic and top basement layers (Smallwood *et al.*, 2001), and direct measurement of gravity gradients may also yield high-resolution information on the sub-basalt structure (Murphy *et al.*, 2002). Other more experimental techniques that may

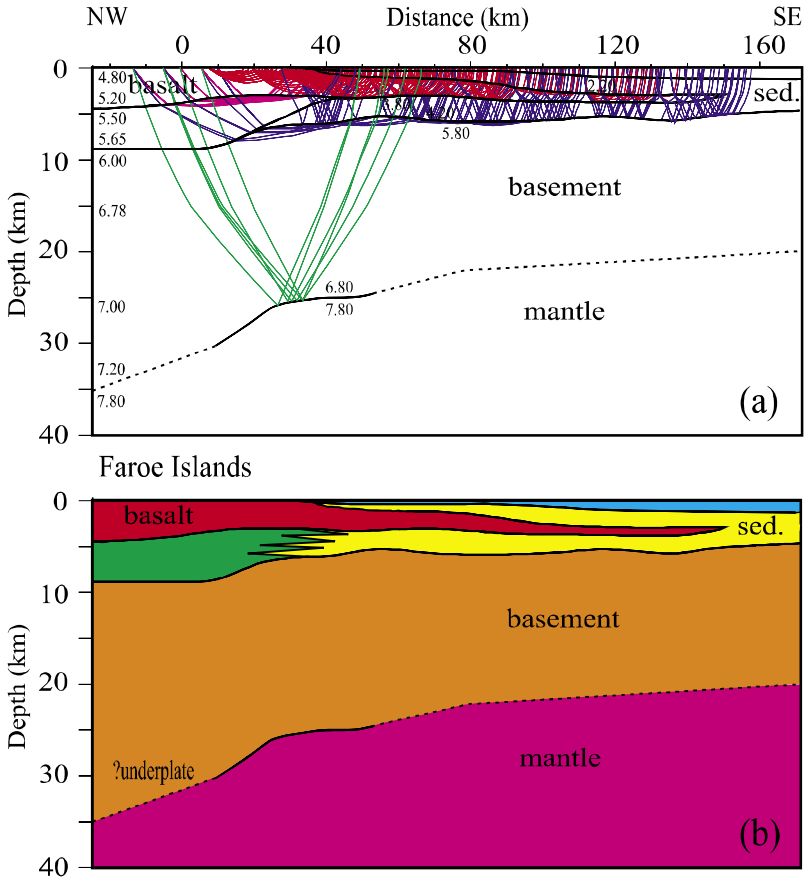

Figure 6. (**a**) Representative wide-angle ray-paths from travel-time tomography through the crustal velocity model along the FLARE-1 profile, including both offshore two-ship data (38 km maximum offset), and onshore land station recording on Suðuroy, which also recorded Moho reflections (for location of FLARE-1 see Figure 1). 0 km is at the projected position of the Lopra well (Figure 1) onto the profile. Red rays are those turned in the basalt layers, or reflected off their bottom. Blue rays are reflected off the top of the basement which marks the base of the sub-basalt sediments, or returned as diving rays through the top of the basement. Green rays are reflections off the Moho. Only every tenth ray is shown for clarity. Selected velocities shown in km/s. (**b**) Interpreted cross-section from the seismic data above, with the extension of the base of the crust across the Faroes shelf extrapolated by gravity modelling from the region where it is constrained by seismic data. Figures modified from Richardson *et al.* (1999).

help show the presence of sub-basalt sediments include controlled source electromagnetic measurements (MacGregor, 2003), seabed compliance measurements (Crawford *et al.*, this volume), and joint inversion of data from different sources such as gravity, MT and seismic (Jegen-Kulcsar and Hobbs, this volume).

Imaging with Wide-Angle Data

Although, as shown in Figure 6, a certain amount of geological interpretation can be obtained from just the 2D velocity field in the subsurface (and this is enhanced if the shear wave velocities and hence the Poisson's ratios of the layers can be determined, because then the rock types are constrained better), an important objective of exploring the geology beneath basalts is to make an image of the sub-basalt region. The recognition of tilted fault blocks, of sills or of structures likely to be of interest as hydrocarbon reservoirs requires knowledge of the shape of reflectors and of the structure of the subsurface. Such images are still obtained most effectively from the nearer-offset reflection data conventionally used for seismic profiling. Unfortunately, even if the energy does penetrate below the basalts, the near-offset images are plagued by the presence of many interbed multiples. Therefore, it is often difficult to know which deep arrivals are primary and which are multiples.

However, the wide-angle data can also be migrated back to normal incidence using pre-stack migration techniques, provided the velocity field is well known (for example from travel-time tomography). If the portion of the wide-angle wavefield outside the water-wave cone that is known to come from the base-basalt reflection is isolated and then is migrated back to normal incidence, this will give a low-resolution image of the shape of the base-basalt reflection (Fliedner and White, 2003). The fact that reflection amplitudes generally increase as the critical angle is approached means that the wide-angle reflections are often very strong, which improves their usefulness for imaging. These migrated wide-angle reflections can then be used to 'tag' which of the many candidate reflections on the profile constructed from the near-offset data is in fact the base-basalt reflection. An example of this is shown in Figure 7, from FLARE profile 2 (see Figure 1 for location). The upper panel (Figure 7a) shows the entire pre-stack depth migrated

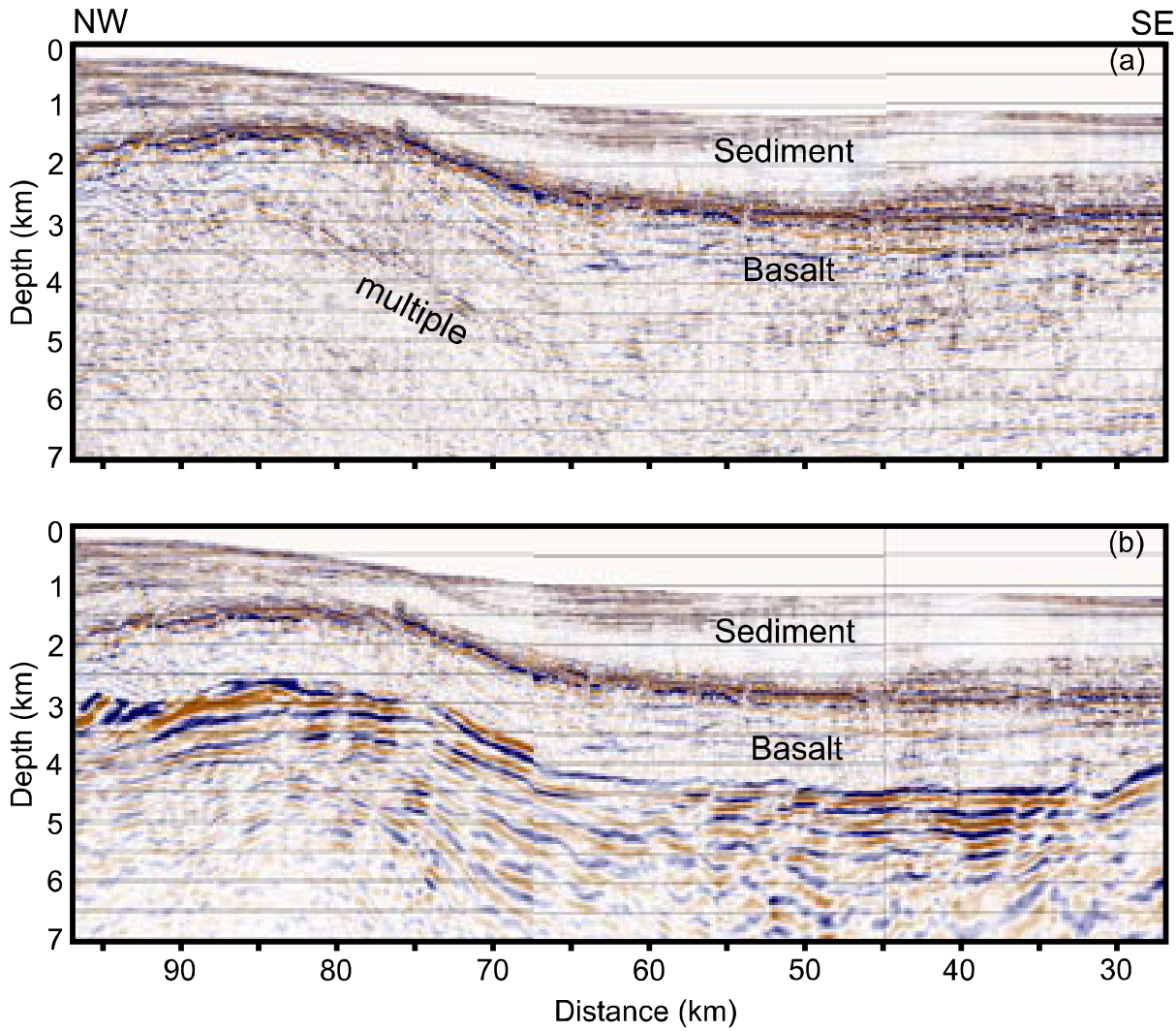

Figure 7. Enlargement of part of FLARE 2 profile (from White *et al.*, 2003), showing (**a**) pre-stack depth migration of the entire seismic dataset, and (**b**) composite image produced by combination of the shallow sediment and top-basalt section with the migrated wide-angle base-basalt arrival. Note the better resolution of the upper panel, but the usefulness of the wide-angle data in the lower panel for identifying which of the candidate reflections in the upper panel is indeed the base-basalt reflector – others are likely to be caused by multiples. See Figure 1 for location.

dataset, complete with many multiples, while the lower panel (Figure 7b) has migrated wide-angle data superimposed. From this it is clear which reflector is from the base-basalt, therefore facilitating interpretation. The technique can be extended to other prominent wide-angle reflections, such as the basement reflector that forms the base to the sub-basalt sediments (Fliedner and White, 2001b), or the prominent wide-angle reflections off the base of the crust (as shown in Figure 4).

Amplitude Modelling and Waveform Inversion

The amplitudes of seismic reflections and refractions contain much more information on the velocity structure than do the travel times alone. In general, the amplitudes are controlled by more local structure than the travel times, because the amplitude of a reflection is affected strongly by the impedance contrast across the reflecting interface, whereas the travel time is the integrated effect of travel along a long path through the entire structure between the source and the receiver. Fliedner and White (2001a) have shown how synthetic seismogram modelling can be used to infer details from wide-angle data of the velocity structure of offshore basalt flows in the Faroes region. Around boreholes, the matching of well log information with surface seismic data is a well-known technique (e.g., for Lopra well, see Christie *et al.*, in press): the frequent observation from such studies

is that while massive single flows can occasionally be identified, the reflectors imaged within basalt sequences are an integrated interference effect of flows on a much finer scale than the seismic wavelength (e.g., Smallwood *et al.*, 1998).

Waveform inversion of the full wide-angle dataset is the obvious next step in constraining the seismic velocity structure along a profile. At present waveform inversion is limited partly by the quality of available data, and partly by the huge computer resources required. In all cases, it is desirable to use a travel-time tomographic method first to find the large-scale velocity structure, and then to use waveform inversion to refine this model. By making simplifying assumptions such as restricting model construction to the acoustic case and ignoring converted energy, or by inverting using a limited number of frequencies in the spectral domain, an inversion scheme can be implemented in a reasonable time using current computer technology (e.g., Pratt, 1999).The ultimate goal remains use of a full elastic model in the waveform inversion (e.g., Shipp and Singh, 2002).

Methods of Recording Long Offsets

Use Long Streamers

The simplest way to record to longer offsets is to tow a longer streamer. Streamer lengths have increased from a typical 2,400 m in the 1970s to a routine 6,000 m and up to 12,000 m for specialist profiles by the end of the 1990s. In the iSIMM survey three streamers were deployed, with a 12,000 m streamer in the centre, and two 4,000 m streamers towed 150 m to either side. This gives a measure of 3D control, particularly on the shallow subsurface structure and on returns scattered from rough surfaces. Relative positioning between the streamers was recorded by acoustic cross-bracing, which allows the three hydrophone streamers to be used to estimate directions of wavefronts moving across the streamer antennae. The fidelity of the detectors within the streamers has also improved over the years, moving from analogue to digital streamers, and in the case of the WesternGeco Q-streamer used for the iSIMM acquisition, to closely spaced (3.125 m) single sensor recording. The 12-km long streamer used for the iSIMM profiles contained 4,000 separately recorded sensors. The advantage of single-sensor recording is that it is possible to use data or noise-adaptive spatial filtering in post-processing after the acquisition to form traces at conventional group intervals (typically 12.5 m or 25 m) with high signal-to-noise ratios for further processing.

With such long streamers it becomes important to know the geometric shape and location of the streamer, which may be pushed sideways behind the ship by the effects of currents and wind. The shape of the streamer behind the ship may be determined by Global Positioning Satellite (GPS) measurements of the locations of buoys at the head and tail of the streamer, together with acoustic cross-bracing and/or magnetic compasses positioned along the streamer.

Use Two Ships

If two seismic vessels are sailed in line astern, a much longer streamer can be synthesised than that towed by a single ship. In the simplest form of this, the trailing ship steams just behind, or alongside the tail buoy of the lead ship, so that the maximum offset is the sum of the two streamers. This has the advantage of there being just one airgun source array, so there is no variation in source along the synthesised streamer, and the shooting ('pop') interval can be as small as in a conventional streamer profile – typically 50 m.

An interesting development of this is to fire airguns alternately from the two ships in a flip-flop firing pattern, in a method first described by Stoffa and Buhl (1979), and by Buhl *et al.* (1982). If the streamers on each ship are the same length, and the trailing ship is two streamer lengths behind the lead ship, then all offsets from zero to three times the streamer length are recorded by this arrangement: so with 6,000 m long streamers, the two ships together can record a profile with offsets up to 18,000 m in a single pass. If multiple passes are made with different ship separations, it is possible to synthesise arbitrarily long streamers. Using this method, the FLARE profiles on the Faroes Shelf acquired data with three passes of two ships to record offsets up to 38,000 m (White *et al.*, 1999).

There are, however, some drawbacks to using two ships to acquire long-offset data. First, the flip-flop shooting means that the fold of coverage is halved compared to single ship firing and

the shot interval is doubled (typically to 100 m). Second, the fact that two different sources and streamers must be used is in itself a disadvantage, since however much care is used in matching the sources and receivers, in practice there will always be some differences which will cause the waveform to vary as different combinations of shots and receivers are used at different offsets. Lastly, because each streamer is liable to feather independently, the assumption of locally 2D structure (i.e. that the structure is invariant perpendicular to the profile) has to be made in the processing. Although such an assumption is inherent in any 2D processing, deviations in the geology from this assumption may lead to discontinuities in the shot gathers calculated from two-ship data which cause worse artefacts in the processing than do the smoothly varying deviations that the same deviations from 2D structure would produce in single-ship data.

Use Ocean Bed Receivers

Offsets to any arbitrary distance, limited only by the power of the seismic source, can be achieved by using fixed seafloor receivers, either in the form of ocean bed cables where the data are fed back to a conventional recording system on a surface ship, or by using autonomous ocean bottom seismometers (OBS). We have already discussed the improved low-frequency bandwidth that is available from ocean bottom receivers (Figure 3c). There is a further considerable advantage of seafloor receivers, which is that 3-component seismometers may be deployed in addition to hydrophones. This enables the direct recording of shear waves, the separation of upgoing and downgoing wavefields by PZ summation (useful for water multiple suppression), and direct measurement of particle motions which may help invert for anisotropy in the subsurface. The disadvantage of seabed recorded data is the spatial inflexibility and relative scarcity of autonomous OBS, and the extra cost of cable-mounted seafloor receivers, which require a second ship.

Along the iSIMM profile, good wide-angle seismic arrivals were recorded by 85 OBS from the entire crust and into the upper mantle out to ranges beyond 140 km (e.g., Figure 4). In the iSIMM project the advantages of long-offset streamer data with their high spatial sampling and fixed OBS data which give better control on the deep structure and on converted waves were combined by recording both types of data along the same profile.

Examples of Sub-Basalt Imaging in Faroes Region using Wide-Angle Profiles

FLARE Example from Two-Ship Data

In Figure 8 we show a crooked-line profile which

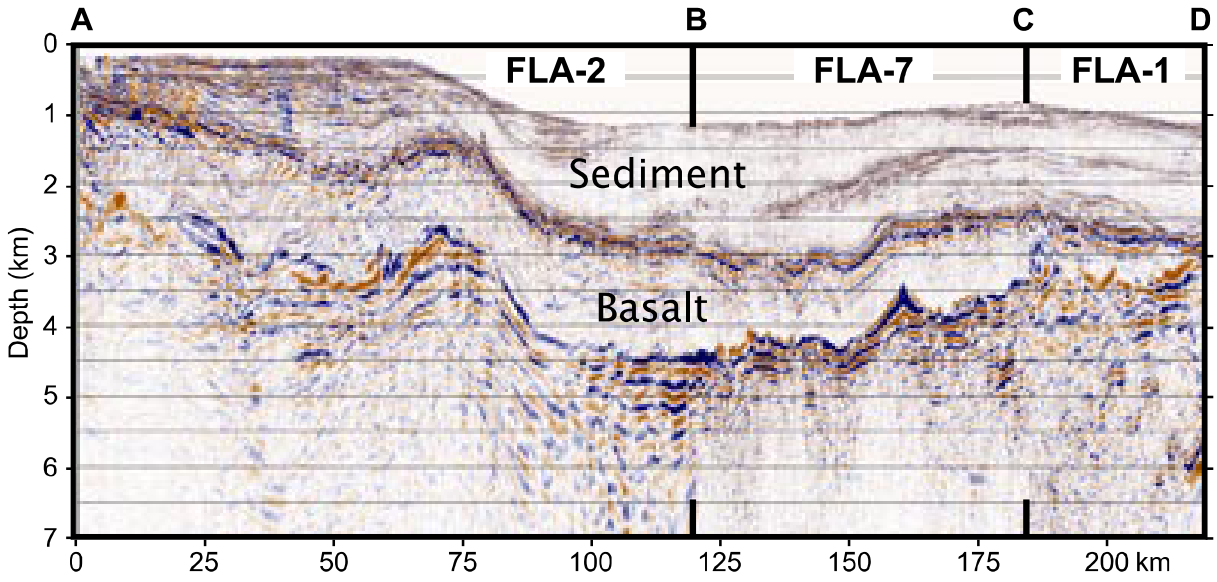

Figure 8. Unfolded seismic section, highlighting the top and base of the basalt flows from FLARE lines 1, 2 and 7 along a transect (shown by red dashes on map in Figure 1, with intersections marked by letters A–D), extending from thick basalts near the Faroe Islands to the feather edge of the sub-surface basalt flows beneath the Faroe-Shetland Trough (from White *et al.*, 2003).

combines sections of FLARE lines 1, 2, and 7 extending from the region of thick basalts near the Faroe Islands to the feather edge of the basalts in the southeast (for location see broken red line on Figure 1). The shallow sedimentary section and the top of the basalt is imaged best using conventional near-offset data. For the deeper section, we have migrated the base-basalt wide-angle reflection and merged it with a pre-stack depth migration of the sediments and top-basalt reflection, as described earlier. It shows good ties at the line intersection points, which gives confidence in the velocity models which were derived independently along each 2D FLARE profile. Note that on the image in Figure 8, the amplitudes of the base-basalt reflection are not directly comparable to those in the shallower section, because we have taken advantage of the high amplitudes of the wide-angle reflections to produce a strong base-basalt image.

The image is often poor where the basalts are thin, because the wide-angle seismic data contain only short segments of reflections from the base of the basalt across a limited range of offsets. Furthermore, diving waves through the basalt are close in travel time to the wide-angle reflections, so they are not easily separated (see Figure 5). Fortunately, in areas of thin basalt, conventional seismic reflection profiles with 6,000 m streamers provide adequate penetration in any case, so the pre-stack depth migration of the long-offset arrivals used in producing our composite image is less important for interpretation where the basalts are thin. By using a mixture of long-offset and conventional seismic profile data, we have been able to map the thickness of the basalts across the Faroes Shelf (Figure 9). Using the same method of migrating the wide-angle reflection at long offsets, but this time choosing the basement arrival (of presumed Cretaceous age), the thickness of the underlying sediment above basement has also been mapped (White *et al.*, 2003).

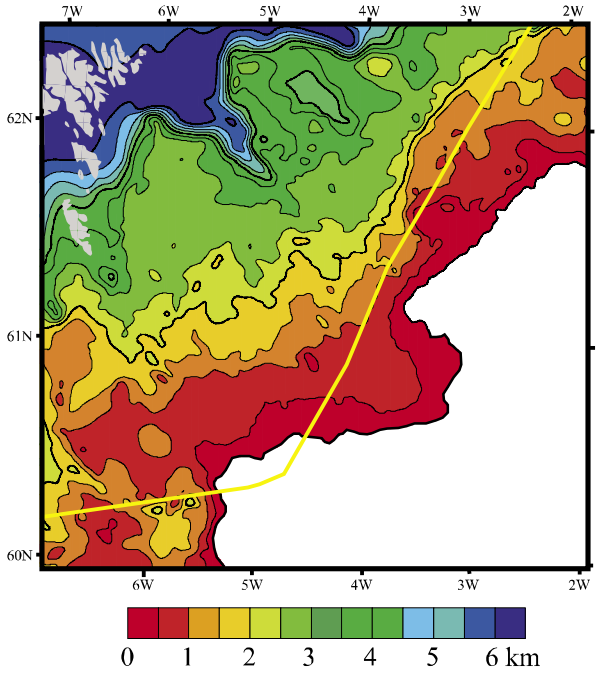

Figure 9. Map of basalt thickness on the Faroes Shelf, using as control the results from FLARE profiles and a large grid of conventional 6-km streamer seismic profiles in the region. The white region in the southeast corner marks the area beyond the feather edge of basalt flows. Map is smoothed, with a contour interval of 500 m. Yellow line marks boundary between UK and Faroese waters. Adapted from White *et al.* (2003).

iSIMM examples from 12-km streamer data

The 400 km long iSIMM seismic profile was acquired using a deep-towed airgun source tuned on the bubble for good low-frequency response (Figure 3d), with a 12-km long streamer. The iSIMM profile extends from the edge of the continental Shetland platform in the southeast to the oceanic crust underlying the Norwegian Sea in the northwest (Figure 10). The profile traverses several distinct provinces, including the stretched continental crust of the Mesozoic Faroe-Shetland Trough, the shallow Fugloy Ridge in the central part of the profile, where basalt flows lie just beneath the seafloor, the volcanic continent-ocean transition created during early Tertiary continental breakup and fully oceanic crust in the northwest. In the Faroe-Shetland Trough, large tilted fault blocks are visible in the basement and extensive igneous sills intrude the sediments. Elsewhere, basalt flows are ubiquitous.

Two extracts of the long iSIMM regional profile are shown in Figures 11 and 12, and discussed below in more detail. They exemplify the different nature of the extrusive volcanism on the continent-ocean margin and on the flank of the Faroes-Shetland Trough. The extract across the continent-ocean transition also demonstrates the seismic response of the lower crustal intrusions and the Moho across the continental margin.

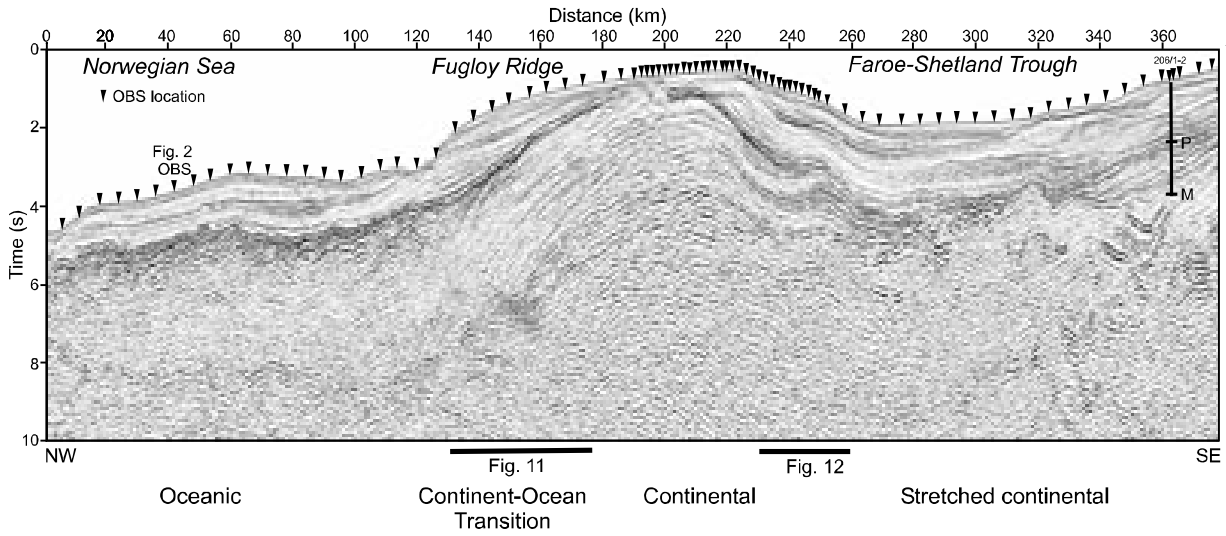

Figure 10. Squash-plot of entire 375 km long iSIMM profile (see Figure 1 for location), after source designature, multiple suppression, and time migration, showing location of hole 206/1-2, which terminates in the Maastrichtian, and of OBS (triangles). P and M mark the tops of the Paleocene and Maastrichtian layers. Data are shown with permission of WesternGeco.

Continent-Ocean Transition

The most prominent feature of the volcanic rocks on the continental margin are the convex-upward, seaward dipping reflectors (SDRs) illustrated in Figure 11. The SDRs are formed by the massive and rapid extrusion of basalts which accompanied continental breakup in the early Tertiary, as a result of interaction between rifting and the thermal anomaly caused by an underlying mantle plume which now lies beneath Iceland (White and McKenzie, 1989). They extend more than 2,500 km along the rifted continental margins in the northern North Atlantic on both the European and Greenland sides. The Faroes region was close to the centre of the mantle plume at the time of breakup, so the melt production here was highest (White and McKenzie, 1989). Hinz (1989) showed that the SDRs were formed by lavas from fissures at the presently down-dip end of the reflectors, which at the time of lava production were elevated by the underlying mantle plume. The lavas originally flowed downhill away from these vents toward the continental hinterland (i.e. toward the right on Figure 11). From borehole sampling of analogous SDRs on the Vøring, Hatton and Edoras Bank margins, they were probably emplaced near sea level (Barton and White, 1997b). The present seaward-dipping, arcuate shape is due to the continued extension of the crust and the loading of the extruded lavas as continental breakup proceeded.

Individual reflectors are coherent over lateral distances of 20 km or more and the entire package of SDRs attains a maximum thickness of 4 km adjacent to the oldest oceanic crust, thickening rapidly from the continental (southeastern) to the oceanic (northwestern) part of the continent-ocean transition. The lateral continuity of the SDRs suggests that the lavas flowed across a flat surface with little topography to impede or channel the flow.

It is probable that the crust in the transition region between continent and ocean was so heavily intruded by the time the SDRs were being formed that it had become hot and ductile, and responded to the ongoing stretching primarily by ductile thinning. The transition region from continent to ocean is very narrow (only a few tens of kilometres wide), which is in marked contrast to non-volcanic margins, where the continental stretching can extend over 250 km width: again this is probably due to the extensive igneous intrusion which so weakened the crust that it focussed further stretching into this narrow, weak region.

The lower part of the continental crust below the SDRs, some 15 km thick, is marked by extensive, strong sub-horizontal reflectivity (Figure 11), with a seismically transparent region between the bottom of the SDRs and the top of the lower-crustal layering. The region of the lower crust with strong layering coincides with abnormally high seismic velocities (above 7.2 km/s) found from the wide-angle OBS analysis. These seismic velocities are markedly higher than the velocities found

in the equivalent portion of lower crust under the adjacent British mainland, and are interpreted as due to the intrusion of mantle-derived magmas during continental breakup (White and McKenzie, 1989). Primitive picritic magmas intruded into the lower crust, rich in iron and magnesium, are likely to have differentiated to produce the less dense, and so more buoyant tholeiitic basalt lavas that were extruded to form the SDRs, leaving behind the denser (and higher seismic velocity) residual in the lower crust. Petrological models suggest that the volume of residual melt left in the lower crust is likely to be two or three times the extruded volume. This is consistent with the relative thicknesses of the lower crust over which prominent layering is seen (interpreted as igneous intrusions), and the thickness of SDRs (interpreted as extruded basalts) (Figure 11), although further detailed seismic analysis is underway to attempt to refine constraints on the percentage of intruded rock in the lower crust.

The lower crustal layering decreases greatly in intensity from the continent-ocean transition to the adjacent oceanic crust to the northwest. This is consistent with the decrease in contrast between physical properties that occur in the lower section of the oceanic crust, where new melt intrudes a mafic crust of similar composition. By contrast, where mafic melts intrude continental crust, there may be a much larger difference in physical properties, and therefore in impedance between the new melts and the pre-existing crust (probably here granitic Lewisian crust), which produces much stronger reflectivity. This probably explains the marked lower crustal reflectivity in the region under the SDRs.

A strong, well-defined reflector at the base of the crust shallows steeply from the continental to the oceanic crust (Figures 10, 11). This reflector is interpreted as marking the Moho discontinuity, based on the strong wide-angle PmP reflections it produces on the OBS (e.g., Figure 4), and the velocities derived from analysis of the OBS arrivals. The 15 km thick oceanic crust adjacent to the continent-ocean transition is considerably thicker than the crust formed above normal oceanic spreading centres away from mantle plumes, but it is consistent with the thickness of the oldest oceanic crust elsewhere on the northern North Atlantic margins (e.g., Barton and White, 1997a; Korenaga *et al.*, 2000; Holbrook *et al.*, 2001), and is thus indicative of raised mantle temperatures caused by the mantle plume at the time of continental breakup.

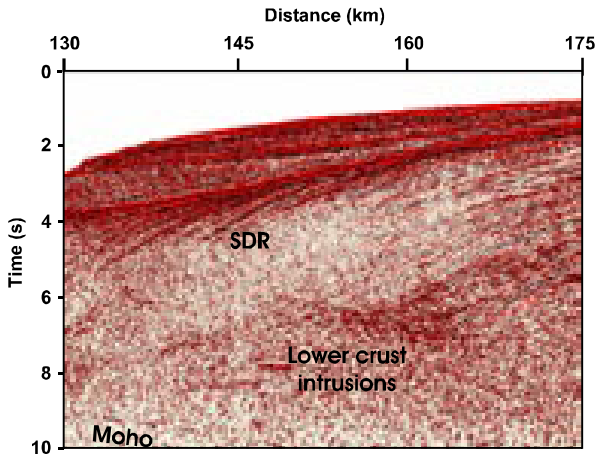

Figure 11. Section of seismic profile crossing the seaward dipping reflector sequence on the continent-ocean boundary (see Figure 10 for location of this 45 km-long extract). Processing includes source designature, multiple suppression and post-stack time migration. Note the superbly imaged SDRs, interpreted as lava flows extruded near sea level from the developing Atlantic rift and flowing landward over the hinterland; the strong lower-crustal layering coincident with high-velocities, presumed to represent lower-crustal intrusions; and the sharp Moho reflection which shallows markedly from continental (southeast) to oceanic (northwest) crust. Data shown with permission of WesternGeco.

Flank of the Faroes-Shetland Trough

The style of extrusive Paleocene volcanic rocks which flowed toward the continental hinterland (which experienced little or no stretching during the Tertiary continental breakup), is quite different from that found at the continent-ocean transition. Figure 12 shows a 30 km extract from the iSIMM seismic profile to illustrate this. The lavas, produced in the volcanically active Atlantic rift to the northwest of this location, flowed up to 150 km landward across a pre-existing and partly sediment-filled landscape toward the Faroe-Shetland Trough, thinning as they flowed (Figure 9). Where they reached the paleo-shoreline, they produced strong, southeastward dipping, sigmoidal reflectors within the basalt sequence. The sigmoidal reflections move upward and southeastward across the section as the lavas progressively built outward, pushing the coastline eastward (Kiørboe, 1999). Strong sub-horizontal layering below the sigmoidal reflectors probably represents early hyaloclastites and lava flows from the first phase of volcanic activity in the Faroes region, while the

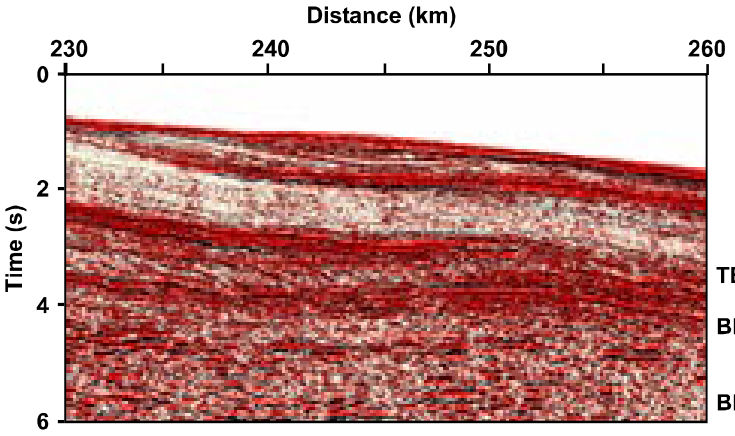

Figure 12. Section of migrated seismic profile crossing the basalt escarpment on the northwestern flank of the Faroe-Shetland Trough (see Figure 10 for location of this 30 km-long extract). Processing includes source designature, multiple suppression and post-stack time migration. Strong sigmoidal foresets are well imaged within the basalt sequence between 3–4 s two-way travel time: these are interpreted as the paleo-coastline in this region when the lavas were extruded. TB – top basalt; BB – base basalt; BM – basement. Data shown with permission of WesternGeco.

equally strong layering above the top of the sigmoidal reflectors is interpreted as due to late lava flows crossing the entire region, capped by lower to middle Eocene and younger sediments. Beneath the bottom of the basalt sequence, lowered velocities measured from the long-offset wide-angle data show the presence of sediments over which the early basalts flowed (Spitzer *et al.*, 2004), with faulted acoustic basement rocks of presumed Cretaceous age beneath them.

Conclusions

Significant improvements to intra- and sub-basalt seismic imaging can be made by careful attention to tuning the source and receiver characteristics so as to optimise the low-frequency response. In the Faroes area, this is shown by the high-quality iSIMM profiles in Figures 10–12. The recording of long-offset data can also provide significant new data, because it is then possible to use the refracted and wide-angle reflected energy outside the water-wave cone both to constrain the velocity distribution in the sub-surface for better pre-stack depth migration, and also for direct imaging using the high-amplitude wide-angle reflections as demonstrated with the FLARE data in Figures 7 and 8. Although the migrated wide-angle reflections are of great value in showing which arrivals are from the base of the basalt, and from deeper in the section, their low frequency content and the large angles at which reflections occur (and therefore the large size of the Fresnel zones), means that they have much poorer resolution than do reflections from closer to normal incidence. So for interpretation purposes it is best to use both a conventional migrated image, together with the composite image that contains the separately identified and migrated high-amplitude wide-angle arrivals which allows us to identify which arrivals are from the deep horizons of interest.

Acknowledgements

The FLARE profiles were shot by Amerada Hess Limited and its partners LASMO (ULX) Limited, Norsk Hydro ASA., DOPAS and Atlantic Petroleum. The iSIMM project is supported by Liverpool and Cambridge Universities, Schlumberger Cambridge Research, Badley Technology Limited, WesternGeco, Amerada Hess, Anadarko, BP, ConocoPhillips, ENI-UK, Statoil, Shell, the Natural Environment Research Council and the Department of Trade and Industry. We thank the Masters and crews of both the *RRS Discovery* and the *M/V Geco Topaz* for their expertise in acquiring high quality datasets for iSIMM. P. Sabel, J-F Hopperstad, A. Harber, A. Langridge and J. Bacon of WesternGeco are thanked for support during the pre-survey modelling and processing of the iSIMM Q-data. We are grateful to M. Fliedner, J. Fruehn and J. Smallwood for their contributions to understanding the FLARE data. University of Cambridge contribution number ES7903.

References

Avedik, F., Renard, V., Allenou, J.P. and Morvan, B. 1993. Single bubble air-gun array for deep exploration. *Geophysics* 58: 366–382.

Barton, A.J. and White, R.S. 1997a. Crustal structure of the Edoras Bank continental margin and mantle thermal anomalies beneath the North Atlantic. *Journal of Geophysical Research* 102: 3109–3129.

Barton, A.J. and White, R.S. 1997b. Volcanism on the Rockall continental margin. *Journal of the Geological Society, London* **154**: 531–536.

Boldreel, L.O. and Andersen, M.S. 1993. Late Paleocene to Miocene compression in the Faeroe-Rockall area. *In*: Parker, J.R. (ed.) *Petroleum Geology of Northwest Europe: Proceedings of the 4th Conference*. Geological Society, London: 1025–1034.

Buhl, P., Diebold, J.B. and Stoffa, P.L. 1982. Array length magnification through the use of multiple sources and receiving arrays. *Geophysics* 47: 311–315.

Christie, P.A.F., Gollifer, I., and Cowper, D. 2002. Borehole seismic results from the Lopra Deepening Project. *Journal of Conference Abstracts* 7(2): 138–139.

Christie, P.A.F., Gollifer, I. and Cowper, D. in press. Borehole seismic studies of a volcanic succession from the Lopra 1/1A borehole in the Faroe Islands, NE Atlantic. *Geology of Denmark Survey Bulletin.*

Crawford, W.C., Singh, S.C., Hulme, T. and Smallwood, J.R. this volume. Applications of seafloor compliance measurements in the Faroes-Shetland Basin. *In*: Ziska, H., Varming, T. and Bloch, D. (eds.) *Faroe Islands Exploration Conference: Proceedings of the 1st Conference, Annales Societatis Scientiarum Færoensis*, Supplementum 43, Tórshavn.

Doré, G., Cartwright, J.A., Stoker, M.S., Turner, J.P. and White, N.J. (eds.) 2002. Exhumation of the North Atlantic Margin: Timing, Mechanisms and Implications for Petroleum Exploration. Geological Society, London, Special Publications 196.

Ebdon, C.C., Granger, P.J., Johnson, H.D. and Evans, A.M. 1995. Early Tertiary evolution and sequence stratigraphy of the Faeroe-Shetland Basin: implications for hydrocarbon prospectivity.*In*: Scrutton, R.A., Stoker, M.S., Shimmield, G.B. and Tudhope,A.W. (eds.) *The Tectonics, Sedimentation and Palaeoceanography of the North Atlantic Region.* Geological Society, London, Special Publications 90: 51–69.

Eldholm, O. and Grue, K. 1994. North Atlantic volcanic margins: dimensions and production rates. *Journal of Geophysical Research* 99: 2955–2988.

Fliedner, M.M. and White, R.S. 2001a. Seismic structure of basalt flows from surface seismic data, borehole measurements and synthetic seismogram modeling. *Geophysics* 66: 1925–1936.

Fliedner, M.M. and White, R.S. 2001b. Sub-basalt imaging in the Faeroe-Shetland Basin with large-offset data. *First Break* 19: 247–252.

Fliedner, M.M. and White, R.S. 2003. Depth imaging basalt flows in the Faeroe-Shetland Basin. *Geophysical Journal International* 152: 353–371.

Fuchs, K. and Müller, G. 1971. Computation of synthetic seismograms with the reflectivity method and comparison with observations. *Geophysical Journal of the Royal Astronomical Society* 23: 417–413.

Hinz, K. 1981. A hypothesis on terrestrial catastrophes: wedges of very thick oceanward dipping layers beneath passive margins – their origin and paleoenvironmental significance. *Geologisches Jahrbuch Reihe* E22: 2–28.

Hoare R., Schearer, P., Langridge, A., Saragoussi, E., Christie, P. and iSIMM Team. this volume. Imaging sub-basalt with deep towed streamer: a case study from the Faroe Islands. *In*: Ziska, H., Varming, T. and Bloch, D. (eds.) *Faroe Islands Exploration Conference: Proceedings of the 1st Conference, Annales Societatis Scientiarum Færoensis*, Supplementum 43, Tórshavn.

Hobbs, R. and Jakubowicz, H. 2000. Marine source signature measurement using a reference seismic source. *Eur. Assn. Geosci. Eng., 62nd Meeting,* Session L0013.

Holbrook, W.S., Larsen, H.C., Korenaga, J., Dahl-Jensen, T., Reid, I.D., Kelemen, P.B., Hopper, J.R., Kent, G.M., Lizarralde, D., Bernstein, S. and Detrick, R.S. 2001. Mantle thermal structure and active upwelling during continental breakup in the North Atlantic. *Earth and Planetary Science Letters* 190: 251–266.

Jacobson, R.S. and Lewis, B.T.R., 1990. The first direct measurements of upper oceanic crustal compressional wave attenuation. *Journal Geophysical Research* 95: 17417–17429.

Japsen, P., Andersen, C., Andersen, H.L., Andersen, M.S., Boldreel, L.O., Mavko, G., Mohammed, N.G., Pedersen, J.M., Petersen, U.K. , Rasmussen, R. , Shaw, F., Springer, N. , Waagstein, R., White, R.S. and Worthington, M. in press. Sub-basalt imaging – new insight from investigations of petrophysical and seismic properties of Faroes basalts (SeiFaBa project). *In*: Doré, A.G. and Vining, B. (eds.) *Petroleum Geology: North-West Europe and Global Perspectives – Proceedings of the 6th Petroleum Geology Conference.* Geological Society, London.

Jegen-Kulcsar, M. and Hobbs, R. this volume. Outline of a joint inversion of gravity, MT and seismic data. *In*: Ziska, H., Varming, T. and Bloch, D. (eds.) *Faroe Islands Exploration Conference: Proceedings of the 1st Conference, Annales Societatis Scientiarum Færoensis*, Supplementum 43, Tórshavn.

Lunnon, Z.C., Christie, P.A.F. and White, R.S. 2003. An evaluation of peak and bubble tuning in sub-basalt seismology: modelling and results. *First Break* 21: 51–56.

Kiørboe, L. 1999. Stratigraphic relationships of the Lower Tertiary of the Faeroe basalt plateau and the Faeroe-Shetland Basin. *In*: Fleet, A.J. and Boldy, S.A.R. (eds.) *Petroleum Geology of Northwest Europe: Proceedings of the 5th Conference*. Geological Society, London: 559–572.

Korenaga, J., Holbrook, W.S., Kent, G.M., Kelemen, P.B., Detrick, R.S., Larsen, H.C., Hopper, J.R. and Dahl-Jensen, T. 2000. Crustal structure of the southeast Greenland margin from joint refraction and reflection seismic tomography. *Journal of Geophysical Research* 105: 21,591–21,614.

MacGregor, L.M. 2003. Joint analysis of marine active and passive source EM data for sub-salt or sub-basalt imaging. *65th Meeting of the European Association of Geoscientists and Engineers, Expanded Abstract*: F18.

Maresh, J., Hobbs, R.W., White, R.S. and Smallwood, J.R. 2003. Attenuation of Atlantic margin basalts using downhole VSP (extended abstract). *73rd Ann. International Meeting: Society of Exploration Geophysicists,* Dallas: 1310–1313.

McBride, J.H., Henstock, T.J., White, R.S. and Hobbs, R.W. 1994. Seismic reflection profiling in deep water: avoiding spurious reflectivity at lower-crustal and upper-mantle traveltimes. *Tectonophysics* 232: 425–435.

Murphy, C.A., Mumaw, G.R. and Stalin, F. 2002. Resolving basalt and sub-basalt geology with high precision, high resolution gravity gradient data. *Journal of Conference Abstracts,* 7(2): 178.

Nadin, P., Kusznir, N.J. and Cheadle M.J. 1997. Early Tertiary plume uplift in the North Sea and Faeroe-Shetland Basin. *Earth and Planetary Science Letters* 148: 109–127.

Naylor, P.H., Bell, B.R., Jolley, D.W., Durnall, P. and Fredsted, R. 1999. Palaeogene magmatism in the Faeroe-Shetland Basin: influences on uplift history and sedimentation. *In*: Fleet, A.J. and Boldy, S.A.R. (eds.) *Petroleum Geology of Northwest Europe: Proceedings of the 5th Conference*. Geological Society, London: 545–558.

Planke, S., 1994. Geophysical response of flood basalts from analysis of wire line logs: Ocean Drilling Program Site 642, Vøring volcanic margin. *Journal of Geophysical Research* 99: 9279–9296.

Pratt, R.G. 1999. Seismic waveform inversion in the frequency domain, Part 1: Theory and verification in a physical scale model. *Geophysics* 64: 888–901.

Pujol, J. and Smithson, S. 1991. Seismic wave attenuation in volcanic rocks from VSP experiments. *Geophysics* 56: 1441–1455.

Richardson, K.R., White, R.S., England, R.W. and Fruehn, J. 1999. Crustal structure east of the Faroe Islands. *Petroleum Geoscience* 5: 161–172.

Roberts, A.W., White, R.S., Lunnon, Z. C., Christie, P. A. F., Spitzer, R. and iSIMM Team. in press. Imaging magmatic rocks on the Faroes margin. *In*: Doré, A.G. and Vining, B. (eds.) *Petroleum Geology: North-West Europe and Global Perspectives - Proceedings of the 6th Petroleum Geology Conference*. Geological Society, London.

Rutledge, J.T. and Winkler, H. 1987. Attenuation measurements in basalt using vertical seismic profile data from the eastern Norwegian Sea. *57th SEG Annual Meeting, New Orleans, USA, Expanded Abstracts* 87: 711–713.

Safar, M.H. 1980. An efficient method of operating the airgun. *Geophysical Prospecting* 28: 85–94.

Shaw, F., Worthington, M.H., Andersen, M.S. and Petersen, U.K. 2004. A study of seismic attenuation in basalt using VSP data from a Faroe Islands borehole (expanded abstract P015). *66th Meeting: European Association of Geoscientists and Engineers*, Paris.

Shipp, R.M. and Singh, S.C. 2002. Two-dimensional full wavefield inversion of wide-aperture marine seismic streamer data. *Geophysical Journal International* 151: 325–344.

Smallwood, J.R., White, R.S. and Staples, R.K. 1998. Deep crustal reflectors under Reydarfjördur, eastern Iceland: Crustal accretion above the Iceland mantle plume. *Geophysical Journal International* 134: 277–290.

Smallwood, J.R., Staples, R.K., Richardson, K.R., White, R.S. and FIRE Working Group. 1999. Crust generated above the Iceland mantle plume: from continental rift to oceanic spreading center. *Journal of Geophysical Research* 104: 22,885–22,902.

Smallwood, J.R., Towns, M.J. and White, R.S. 2001. The structure of the Faroe-Shetland Trough from integrated deep seismic and potential field modelling. *Journal of the Geological Society, London* 158: 409–412.

Smallwood, J.R. and Maresh, J. 2002. The properties, morphology and distribution of igneous sills: Modelling, borehole data and 3D seismic from the Faroe-Shetland area. *In:* Jolley, D.W. and Bell, B.R. (eds.) *The North Atlantic Igneous Province: stratigraphy, tectonic, volcanic and magmatic processes.* Geological Society, London, Special Publications 197: 271–306.

Sørensen, A.B. 2003. Cenozoic basin development and stratigraphy of the Faroes area. *Petroleum Geoscience* 9: 189–207.

Spitzer, R., White, R.S., Christie, P.A.F. and iSIMM Group 2004. Sub-basalt imaging along the iSIMM profile – integration of surface and ocean bottom seismic data (expanded abstract D042). *66th Meeting: European Association of Geoscientists and Engineers*, Paris.

Staples, R.K., Hobbs, R.W. and White, R.S. 1999. A comparison between airguns and explosives as wide-angle seismic sources. *Geophysical Prospecting* 47: 313–339.

Stoffa, P.L. and Buhl, P.1979. Two-ship multichannel seismic experiments for deep crustal studies: Expanding spread and constant offset profiles. *Journal of Geophysical Research* 84: 7645–7660.

Toksöz, M.N., Johnston, D.H. and Timur, A. 1979. Attenuation of seismic waves in dry and saturated rocks: I. Laboratory measurements. *Geophysics* 44: 681–690.

Waagstein, R. 1988. Structure, composition and age of the Faeroe basalt plateau. *In*: Morton, A.C. and Parson, L.M. (eds.) *Early Tertiary Volcanism and the Opening of the NE Atlantic*. Geological Society, London, Special Publications 39: 225–238.

White, N.J. and Lovell, B. 1997. Measuring the pulse of a plume with the sedimentary record. *Nature* 387: 888–891.

White, R. and McKenzie, D. 1989. Magmatism at rift zones: The generation of volcanic continental margins and flood basalts. *Journal of Geophysical Research* 94: 7685–7729.

White, R.S., McBride, J.H., Maguire, P.K.H., Brandsdóttir, B., Menke, W.H., Minshull, T.A., Richardson, K.R., Smallwood, J.R., Staples, R.K. and the FIRE Working Group. 1996. Seismic images of crust beneath Iceland contribute to long-standing debate. *EOS* 77: 197 and 200–201.

White, R.S., Fruehn, J., Richardson, K.R., Cullen, E., Kirk, W., Smallwood, J.R. and Latkiewicz, C. 1999. Faroes Large Aperture Research Experiment (FLARE): Imaging through basalts, in Fleet, A.J. and Boldy, S.A.R. (eds.) *Petroleum Geology of Northwest Europe: Proceedings of the 5th Conference*. Geological Society, London: 1243–1252.

White, R.S., Christie, P.A.F., Kusznir, N.J., Roberts, A., Hurst, N., Lunnon, Z., Parkin, C.J., Roberts, A.W., Smith, L.K., Spitzer, R., Surendra, A. and Tymms, V. 2002. iSIMM pushes frontiers of marine seismic acquisition. *First Break* 20: 782–786.

White, R.S., Smallwood, J.R., Fliedner, M.M., Boslaugh, B., Maresh, J. and Fruehn, J. 2003. Imaging and regional distribution of basalt flows in the Faroe-Shetland Basin. *Geophysical Prospecting* 51: 215–231.

Ziolkowski, A., Parkes, G., Hatton, L. and Haugland, T.

1982. The signature of an air-gun array – Computation from near-field measurements including interactions. *Geophysics* 47: 1413–1421.

Ziolkowski, A., Hanssen, P., Gatliff, R., Jakubowicz, H., Dobson, A., Hampson, G., Li, X.-Y. and Liu, E. 2003. Use of low frequencies for sub-basalt imaging. *Geophysical Prospecting* 51: 169–182.